OPTICALLY VISUALIZED SOUND FIELD RECONSTRUCTION BASED ON SPARSE SELECTION OF POINT SOUND SOURCES

Kohei Yatabe and Yasuhiro Oikawa

Department of Intermedia Art and Science, Waseda University, Tokyo, Japan

ABSTRACT

Visualization is an effective way to understand the behavior of a sound field. There are several methods for such observation including optical measurement technique which enables a non-destructive acoustical observation by detecting density variation of the medium. For audible sound propagating through the air, however, smallness of the variation requires high sensitivity of the measuring system that causes problematic noise contamination. In this paper, a method for reconstructing two-dimensional audible sound fields from noisy optical observation is proposed.

Index Terms— Sound field visualization, sparse approximation, Kirchhoff–Helmholtz integral equation, convex optimization.

1. INTRODUCTION

Understanding the behavior of a sound field is one of the most important tasks for many acousticians. For this purpose, one highly effective way is to visualize it.

A microphone array is the standard choice for such observation. However, it is effortful to obtain detailed information over a broad area. In addition, the presence of measuring instruments inside a sound field changes the field itself.

As the powerful alternative, optical measurement methods, which enable a contactless non-destructive acoustical observation, are studied for some decades mainly in the field of ultrasonic and underwater acoustics [1,2]. Roughly speaking, these methods detect acoustical information through density variation of a medium caused by sound. Ordinary situation for radiating ultrasonic and underwater sound enforces relatively high density variation, and thus optical methods are friendly with those areas.

However, audible sound passing through the air is hard to detect by optics due to its smallness of the pressure variation. The fact that only a few articles can be found on this topic is reflecting the difficulty of the situation [3–16]. Audible sound requires exceedingly high sensitivity of the optical system for the detection, which leads to striking noise contamination. Ordinarily, averaging of multiple observations, a time consuming process, is performed to deal with it.

In the previous paper [17], we proposed a reconstruction method for an optically visualized two-dimensional sound field. It is based on the boundary integral equation (BIE) with the Helmholtz equation constraint, which may overfit to noisy data through evanescent components. In order to eliminate such an unrealistic solution, further assumption is needed.

It is natural to assume that there are few sound sources, which can be well approximated by point sources, around the observing region. This assumption leads to a sparse estimation problem which is proved to be highly effective for many signal processing problems [18,19]. In this paper, a sparse reconstruction method for a noisy two-dimensional sound field utilizing BIE and point sound sources is proposed.

2. OPTICAL OBSERVATION OF A SOUND FIELD

In the linear acoustics, the refractive index of the air n can be approximated as a function of the sound pressure p:

$$n = n_0 + \frac{n_0 - 1}{\gamma p_0} p, \tag{1}$$

where n_0 and p_0 are the refractive index and the pressure under standard atmospheric conditions, and γ is the specific heat ratio. Therefore, measuring the refractive index of the air, using optical measurement devices, enable us to know the sound pressure at the corresponding points in a contactless way.

Let us assume that a measuring light beam is passing in the x_3 direction. Then, for instance, a laser Doppler vibrometer (LDV) [3, 12] measures phase ϕ of the measuring light beam, which contains information of the refractive index in the form

$$\phi = k_0 \int n \, dx_3, \tag{2}$$

where k_0 is the wave number of the light in vacuum. For another example, the Schlieren method [15] can measure the light deflection angle ε_j in the x_j $(j = 1, 2)$ direction, which corresponds to the gradient of the refractive index as

$$\varepsilon_j = \frac{1}{n_0} \int \frac{\partial n}{\partial x_j} \, dx_3. \tag{3}$$

Thus, it is able to measure the sound pressure or the particle velocity of a sound field from these optical methods. There are several other methods utilizing different optical phenomena such as diffraction [9, 10], and back-scattering [20].

3. OPTICALLY VISUALIZED SOUND FIELD RECONSTRUCTION

As in the previous section, the optical methods enables a contactless acoustical measurement. However, quantitative assessment using these methods is relatively difficult for the following reasons: (1) measured quantity is integrated along the light beam that conceals point-wise information; and (2) sound related variation of the refractive index is quite small comparing to other phenomena such as thermal fluid that leads to severe noise contamination. In this paper, we will focus on the latter problem for better visualization.

3.1. Helmholtz equation and its boundary integral form

Let us assume that a two-dimensional visualized sound field in the observing region Ω is governed by the homogeneous Helmholtz equation:

$$\left(\triangle + k^2\right) u(x, \omega) = 0, \tag{4}$$

where $x \in \Omega \subset \mathbb{R}^2$, $\triangle = \sum_j \partial^2 / \partial x_j^2$, $k = \omega/c$ is the wave number, ω is the angular frequency, and c is the speed of sound. Its boundary integral form is obtained as

$$u(x) = \int_{\partial \Omega} \left[\Phi(x, y) \frac{\partial u(y)}{\partial \nu_y} - \frac{\partial \Phi(x, y)}{\partial \nu_y} u(y) \right] dS(y), \tag{5}$$

where $\partial\Omega$ is the boundary of Ω, $y \in \partial\Omega$, ν_y is an outward-pointing unit normal vector at y,

$$\Phi(x, y) = \frac{i}{4} H_0^{(1)}(k|x - y|) \tag{6}$$

is the fundamental solution for the two-dimensional Helmholtz equation, $|\cdot|$ is the Euclidean distance, $i = \sqrt{-1}$, and $H_0^{(1)}$ is the Hankel function of the first kind of order 0. We omitted the symbol ω from Eq. (5) as $u(x) = u(x, \omega)$ for ease. Note that the solution $u(x, \omega)$ can be converted to the time domain solution $u(x, t)$ using the (inverse) Fourier transform.

3.2. Least squares formulation of the previous work [17]

Let Eq. (5) be shortly represented by the integral operator K as $u(x) = (Ku)(x)$. Then the method in the previous paper [17] can be written as

$$\begin{aligned} \underset{u}{\text{minimize}} \quad & \sum_m \left| p(x_m) - (Ku)(x_m) \right|^2 \\ \text{subject to} \quad & \left(\triangle + k^2\right) u(y) = 0 \end{aligned} \tag{7}$$

where $p(x_m)$ is the measured data at x_m. This boundary condition estimation problem utilized the BIE as a physical model to fit in the data in the sense of minimum square error. The ill-posedness of the problem was reduced by the Helmholtz equation constraint which requires the solution to be a sound. However, this constraint cannot restrict the solution space to the subspace where the actual sound field lies. While the BIE assumes that no sound source exists inside Ω, the Helmholtz equation constraining u at $\partial\Omega$ does not.

3.3. Subspace where the true solution lies

The true boundary condition can be represented as

$$u(y) = \int_{\mathbb{R}^2 \setminus B(o;a)} C(z) \, H_0^{(1)}(k|y - z|) \, dz, \tag{8}$$

$$\frac{\partial u(y)}{\partial \nu_y} = \int_{\mathbb{R}^2 \setminus B(o;a)} k \, C(z) \, H_1^{(1)}(k|y - z|) \frac{\partial |y - z|}{\partial \nu_y} dz, \tag{9}$$

where C is a complex coefficient depending on the position, a is the radius of a region where any sound source does not exist, $\Omega \subset B(o; a) \subset \mathbb{R}^2$, and $B(o; a)$ is the open ball with radius a centered at o. Therefore, the estimation problem should be constrained by Eqs. (8) and (9).

3.4. Proposed method

Assuming that the integrations in Eqs. (8) and (9) can be approximated well by finite sum, a family of functions

$$\psi_{n,\ell}(y) = H_0^{(1)}\Big(k \, \Big| \, y - (a + r_0^\ell) \begin{bmatrix} \cos \frac{2\pi n}{N} \\ \sin \frac{2\pi n}{N} \end{bmatrix} \Big| \Big) \tag{10}$$

is introduced, where $n = 1, 2, \ldots, N$, and $\ell \in I \subset \mathbb{Z}$. This set of functions represents the boundary condition at the point y on the boundary $\partial\Omega$ generated by each point source.

Discretization of the square error function in Eq. (7) obtains

$$\min_{\mathbf{u}} \, \left\| \mathbf{p} - \mathbf{K}\mathbf{u} \right\|_2^2 \tag{11}$$

where

$$\mathbf{p} = [\, p(x_1) \; p(x_2) \; \cdots \; p(x_M)]^T,$$

$$\mathbf{K} = [\, \boldsymbol{\Phi} \; -\boldsymbol{\Phi}'], \quad \boldsymbol{\Phi}_{ij} = \Phi(x_i, y_j), \quad \boldsymbol{\Phi}'_{ij} = \frac{\partial \Phi(x_i, y_j)}{\partial \nu_{y_j}},$$

$$\mathbf{u} = [\, \frac{\partial u(y_1)}{\partial \nu_{y_1}} \; \cdots \; \frac{\partial u(y_D)}{\partial \nu_{y_D}} \; u(y_1) \; \cdots \; u(y_D)]^T, \tag{12}$$

and $\| \cdot \|_p$ denotes ℓ_p-norm. According to Eqs. (8) and (9), $\mathbf{u}$ should be represented by a linear combination of $\psi_{n,\ell}$ as

$$\mathbf{u} = \boldsymbol{\Psi}\mathbf{x}, \tag{13}$$

where

$$\boldsymbol{\Psi} = [\, \mathbf{D}^T \, \mathbf{D}'^T]^T, \quad \mathbf{D}_{ij} = \psi_{n_j, \ell_j}(y_i), \quad \mathbf{D}'_{ij} = \frac{\partial \psi_{n_j, \ell_j}(y_i)}{\partial \nu_{y_i}},$$

$$\mathbf{x} = [\, C_1 \; C_2 \; \cdots \; C_{NL}]^T. \tag{14}$$

Then, we propose a sparse reconstruction method by solving the following LASSO problem:

$$\min_{\mathbf{x}} \, \left\| \mathbf{p} - \mathbf{K}\boldsymbol{\Psi}\mathbf{x} \right\|_2^2 + \lambda \|\mathbf{x}\|_1, \tag{15}$$

which can be extended to a method utilizing several boundaries

$$\min_{\mathbf{x}} \, \sum_n \left\| \mathbf{p} - \mathbf{K}_n \boldsymbol{\Psi}_n \mathbf{x} \right\|_2^2 + \lambda \|\mathbf{x}\|_1, \tag{16}$$

where $\lambda > 0$ is a regularization parameter which should be chosen depending on the noise level of observed data. The procedure of the proposed method is as follows:

1. Import measured data **p** and its spatial setting.
2. Create **K** and **Ψ** as in Eqs. (12) (14) from Eqs. (6) (10).
3. Solve Eq. (15) or (16) to estimate the coefficients **x**.
4. Calculate the boundary condition **u** from estimated **x** by Eq. (13) and information at any points inside the region using Eq. (5).

Note that all vectors and matrices in Eqs. (15) and (16) are composed of complex valued elements. Thus, a special care is needed for solving them [21]. In this paper, we utilized the alternating direction method of multiplier (ADMM) [22] with real domain mapping [23].

4. EXPERIMENTS

4.1. Numerical simulation

In order to confirm effectiveness of the proposed method, numerical experiments were performed. The simulation setting is shown in Table 1. ℓ_2-norm and ℓ_4-norm ball shaped boundaries were placed around the visualized sound field sampled by 16×16 sampling points as in Fig. 1. $\psi_{n,\ell}$ surrounding the boundaries are plotted also in the figure.

For the quantitative evaluation, the signal-to-noise ratio (SNR) of reconstructed sound fields

$$\text{SNR}_{\text{result}} = 10 \log_{10} \frac{\sum |p|^2}{\sum |p - \hat{p}|^2}, \quad (17)$$

where p is the sound pressure of the original sound field and $\hat{p}$ is the reconstructed sound field, was calculated. The experiments were performed for several observed data whose SNR

$$\text{SNR}_{\text{data}} = 10 \log_{10} \frac{\sum |p|^2}{\sum |w|^2}, \quad (18)$$

where w denotes Gaussian noise, was arbitrarily chosen by adjusting the level of the noise.

Table 1. Simulation condition.

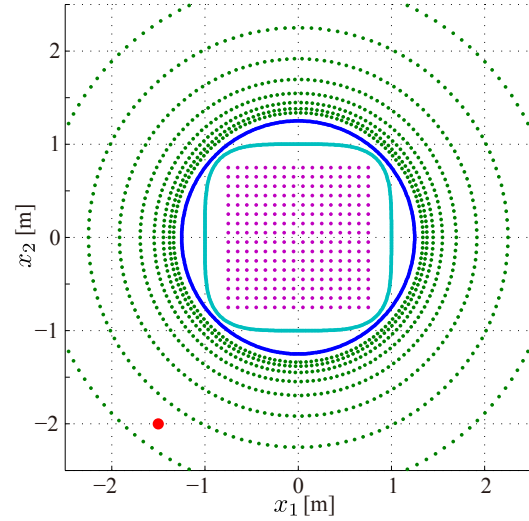| Sampling points	$16 \times 16 \ (= 256)$ points
Sound source position	$(-1.5, -2)$
# disc. points on boundary	512
Parameters in Eq. (10)	$N = 150, \quad r_0 = 1.5$ m
ℓ in Eq. (10)	$\ell = -6, \ldots, 12$
Regularization parameter	$\lambda = 2^{-14}$
Sampling points interval	0.1 m
Sound speed	$c = 340$ m/s
Spatial Nyquist frequency	1700 Hz

Fig. 1. Setting of the sampling points (purple), boundaries (blue, light green), $\psi_{n,\ell}$ (dark green), and a point sound source (red) for the numerical simulation in Section 4.1. The boundary written in the blue circle was used for both estimation and reconstruction, while the light green ℓ_4-norm ball shaped boundary was used only for the penalty.
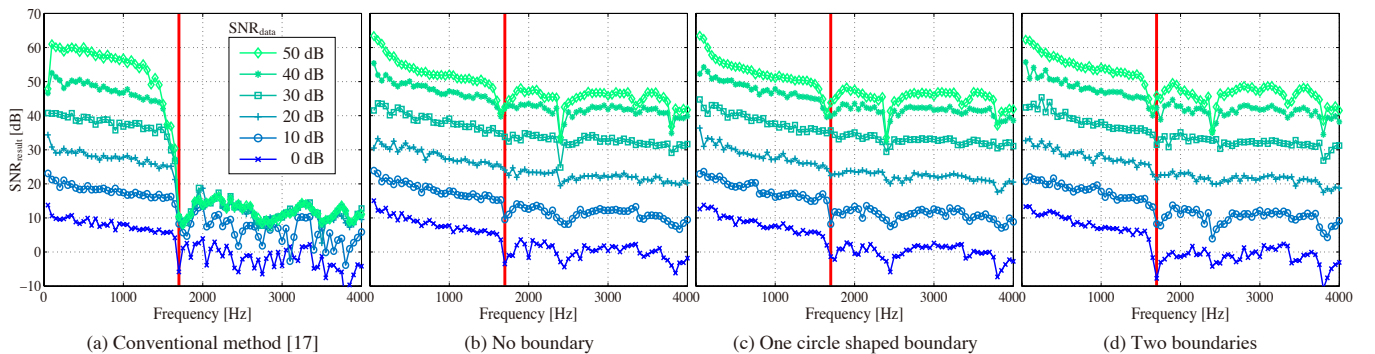

(a) Conventional method [17]   (b) No boundary   (c) One circle shaped boundary   (d) Two boundaries

Fig. 2. Experimental result for the numerical experiment in Section 4.1. Each color represents the SNR of the original data **p** which was calculated from $16 \times 16 = 256$ samples, while the vertical axis represents the SNR of reconstructed sound fields calculated from $301 \times 301 = 90601$ samples. (a) shows the result for the conventional method in [17]. (c), and (d) illustrates the result for the proposed method where the number of boundaries used for the estimation were different. (b) is calculated for comparison to examine the effect of the boundaries. The vertical red lines indicate the spatial Nyquist frequency of the sampling points.

Table 2. Measurement condition.

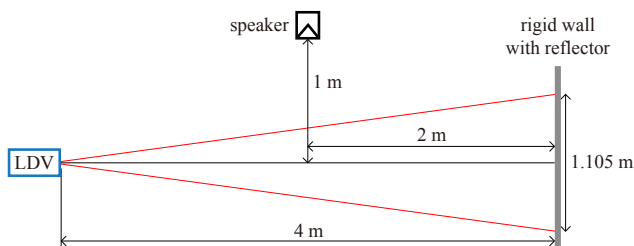| Place for measurement	Huge rectangular room @Waseda Univ. Honjo campus
Loud speaker	Yamaha MSP5 studio
Scanning LDV	Polytec PSV-300
Measured points	25×25 (= 625) points

Fig. 3. Measurement setup of the LDV and a sound source. The wall reflecting the laser emitted from the LDV is made of cement with more than 30 cm thickness. The size of the room is 12 m×20 m×6.5 m.

Figure 2 shows the SNR of the reconstruction results versus frequencies of the sound fields. Each color represents the SNR of the original data (SNR$_{\text{data}}$) which was calculated from $16 \times 16 = 256$ sampling points whereas the vertical axis (SNR$_{\text{result}}$) was calculated from $301 \times 301 = 90601$ reconstructed points. The red lines indicate the spatial Nyquist frequency for the sampling points obtaining the original data.

From the results, it can be confirmed that the proposed method can estimate the original field from sparsely observed data even when the frequencies of the sound field exceed the spatial Nyquist frequency, while the conventional method cannot due to the overfitting. It can also be confirmed that when the number of boundary had increased, the reconstruction results became slightly better. This phenomena should

be the result of restriction of the degrees of freedom of the model caused.

In this experiment, the regularization parameter was fixed to $\lambda = 2^{-14}$ for all situations. The result for high SNR data became better when the parameter was set lower, and that of low SNR data was better with a higher value of the parameter. In practice, λ should be tuned for each noise level.

4.2. Application to real data

The proposed method was applied to the real data obtained by an LDV [3]. The measurement condition and setup are illustrated in Table 2 and Fig. 3. The scanning LDV emitted a laser beam to each point on the light reflector stuck on the thick rigid cement wall of the huge (12 m × 20 m × 6.5 m) rectangular room. The sound source was obtained by multiplying four periods of 4000 Hz sinusoidal wave with the Hann window.

Figure 4 shows the reconstruction result. It is hard to confirm the pulse from the raw data visually due to measurement noise. On the contrary, the proposed method can clearly depict the sound. This result indicate that the proposed method can ignore noisy phenomenon which does not behave as sound physically.

5. CONCLUSION

In this paper, a reconstruction method for an optically visualized sound field was proposed. The proposed method effectively formulates the reconstruction problem as the LASSO problem with the family of functions whose linear combination gives a solution lying in the space of the true solutions.

Future works include finding a condition for choosing appropriate r_0, N, and I for $\psi_{n,\ell}$. Moreover, the guideline for choosing the shape, position, and number of the boundaries should be investigated. Furthermore, reconstruction of three-dimensional sound pressure distribution from optically measured data will be considered.
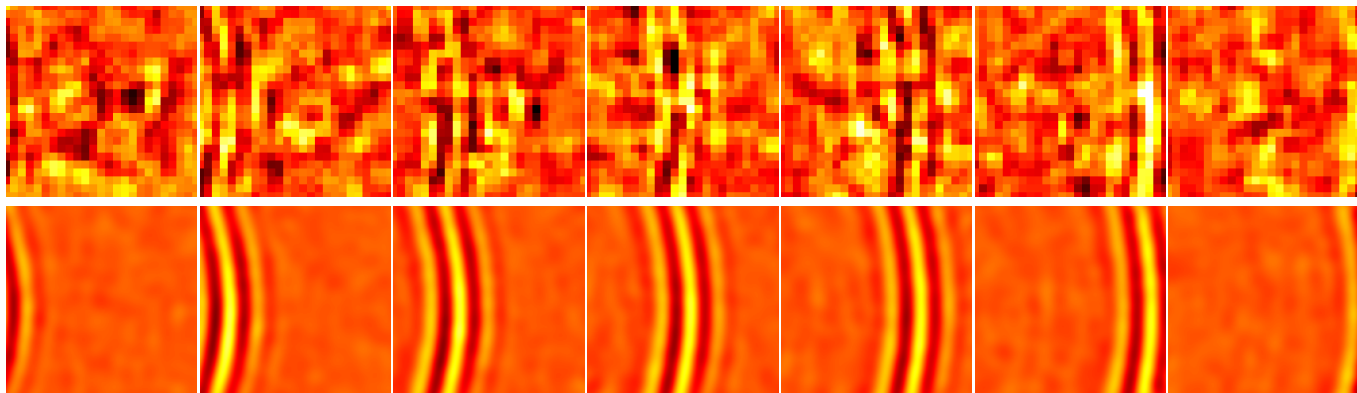

Fig. 4. Reconstruction of a non-stationary field measured by an LDV. The measurement condition is listed in Table 2. The sound source was a pulse generated by multiplying 4 periods of 4000 Hz sinusoidal wave with the Hann window. The upper row shows the original measured data while the lower row shows the reconstructed results obtained by the proposed method.

6. REFERENCES

[1] J.A. Bucaro and H.D. Dardy, "Visualization of ultrasonic waves in air," *J. Acoust. Soc. Am.*, vol. 62, no. 6, pp. 1506–1507, Dec. 1977.

[2] A.R. Harland, J.N. Petzing, and J.R. Tyrer, "Nonperturbing measurements of spatially distributed underwater acoustic fields using a scanning laser Doppler vibrometer," *J. Acoust. Soc. Am.*, vol. 115, no. 1, pp. 187–195, Jan. 2004.

[3] Y. Oikawa, M. Goto, Y. Ikeda, T. Takizawa, and Y. Yamasaki, "Sound field measurements based on reconstruction from laser projections," in *Int. Conf. Acoust., Speech Signal Process. (ICASSP)*. IEEE, Mar. 2005, vol. IV, pp. 661–664.

[4] Y. Ikeda, M. Goto, N. Okamoto, T. Takizawa, Y. Oikawa, and Y. Yamasaki, "A measurement of reproducible sound field with laser computed tomography (in japanese)," *J. Acoust. Soc. Jpn.*, vol. 62, no. 7, pp. 491–499, Jul. 2006.

[5] Y. Ikeda, N. Okamoto, M. Goto, T. Konishi, Y. Oikawa, and Y. Yamasaki, "Error analysis for the measurement of sound pressure distribution by laser tomography (in japanese)," *J. Acoust. Soc. Jpn.*, vol. 64, no. 1, pp. 3–7, Jan. 2008.

[6] Y. Ikeda, N. Okamoto, T. Konishi, Y. Oikawa, Y. Tokita, and Y. Yamasaki, "Observation of traveling wave with laser tomography (in japanese)," *J. Acoust. Soc. Jpn.*, vol. 64, no. 3, pp. 142–149, Mar. 2008.

[7] Y. Oikawa, T. Hasegawa, Y. Ouchi, Y. Yamasaki, and Y. Ikeda, "Visualization of sound field and sound source vibration using laser measurement method," in *20th Int. Congr. Acoust. (ICA)*, Aug. 2010, vol. 898.

[8] S. Frank and J. Schell, "Sound field simulation and visualisation based on laser Doppler vibrometer measurements," in *Forum Acusticum*, 2005, pp. 91–97.

[9] Y. Sonoda, "Direct detection of acoustic waves by laser light diffraction and proposals of the optophone," in *16th Int. Congr. Acoust. (ICA)*, June 1998, vol. 1, pp. 427–428.

[10] Y. Sonoda and Y. Nakazono, "Development of optophone with no diaphragm and application to sound measurement in jet flow," *Advances Acoust. Vib.*, vol. 2012, no. 909437, pp. 1–17, 2012.

[11] T. Sakoda and Y. Sonoda, "Visualization of sound field with uniform phase distribution using laser beam microphone coupled with computerized tomography method," *Acoust. Sci. & Tech.*, vol. 29, no. 4, pp. 295–299, Jul. 2008.

[12] A. Torras-Rosell, S. Barrera-Figueroa, and F. Jacobsen, "Sound field reconstruction using acousto-optic tomography," *J. Acoust. Soc. Am.*, vol. 131, no. 5, pp. 3786–3793, May 2012.

[13] A. Torras-Rosell, S. Barrera-Figueroa, and F. Jacobsen, "An acousto-optic beamformer," *J. Acoust. Soc. Am.*, vol. 132, no. 1, pp. 144–149, July 2012.

[14] B.H. Pandya, G.S. Settles, and J.D. Miller, "Schlieren imaging of shock waves from a trumpet," *J. Acoust. Soc. Am.*, vol. 114, no. 6, pp. 3363–3367, Dec. 2003.

[15] M.J. Hargather, G.S. Settles, and M.J. Madalis, "Schlieren imaging of loud sounds and weak shock waves in air near the limit of visibility," *Shock Waves*, vol. 20, no. 1, pp. 9–17, Feb. 2010.

[16] R. Malkin, T. Todd, and D. Robert, "A simple method for quantitative imaging of 2D acoustic fields using refracto-vibrometry," *J. Sound Vib.*, vol. 333, no. 19, pp. 4473–4482, Sept. 2014.

[17] K. Yatabe and Y. Oikawa, "PDE-based interpolation method for optically visualized sound field," in *Int. Conf. Acoust., Speech Signal Process. (ICASSP)*. IEEE, May. 2014, pp. 4771–4775.

[18] Y. Oikawa and Y. Yamasaki, "Direction of arrival estimation using matching pursuit and its application to source separation for convolved mixtures," *Acoust. Sci. & Tech.*, vol. 26, no. 6, pp. 486–494, 2005.

[19] S. Koyama, S. Shimauchi, and H. Ohmuro, "Sparse sound field representation in recording and reproduction for reducing spatial aliasing artifacts," in *Int. Conf. Acoust., Speech Signal Process. (ICASSP)*. IEEE, May 2014, pp. 4443–4447.

[20] K. Ishikawa, Y. Oikawa, and Y. Yamasaki, "Backscattering measurement method for sound field using pulsed laser," in *Forum Acusticum*. EAA, Sept. 2014.

[21] T. Adali and P. Schreier, "Optimization and estimation of complex-valued signals: Theory and applications in filtering and blind source separation," *IEEE Signal Process. Mag.*, vol. 31, no. 5, pp. 112–128, Sept. 2014.

[22] S. Boyd, N. Parikh, E. Chu, B. Peleato, and J. Eckstein, "Distributed optimization and statistical learning via the alternating direction method of multipliers," *Found. Trends Mach. Learning*, vol. 3, no. 1, pp. 1–122, July 2011.

[23] T. Mizoguchi and I. Yamada, "An algebraic translation of cayley-dickson linear systems and its applications to online learning," *IEEE Trans. Signal Process.*, vol. 62, no. 6, pp. 1438–1453, Mar. 2014.